

Coverage-dependent hydrogen adsorption site determination on Rh(100) by high-resolution core-level spectroscopy

E. Vesselli,^{1,2} A. Baraldi,^{1,2} F. Bondino,² G. Comelli,^{1,2} M. Peressi,^{3,4} and R. Rosei^{1,2}¹*Physics Department and Center of Excellence for Nanostructured Materials, Università degli Studi di Trieste, via A. Valerio 2, 34127 Trieste, Italy*²*Laboratorio Nazionale TASC-INFN, Area Science Park, S.S. 14 km 163.5, 34012 Basovizza (Trieste), Italy*³*Dipartimento di Fisica Teorica, Università degli Studi di Trieste, Strada Costiera 11, 34014 Trieste, Italy*⁴*INFN-DEMOCRITOS National Simulation Center, Trieste, Italy*

(Received 13 October 2003; revised manuscript received 28 April 2004; published 8 September 2004)

We show that high-resolution real-time x-ray photoelectron spectroscopy can be used to determine hydrogen adsorption sites as a function of coverage on Rh(100). The measurement of the surface core-level shifts does not suffer from the lack of direct sensitivity of other surface probes due to the low scattering cross section and high mobility of atomic hydrogen. At low temperatures (70–140 K) and coverage (below 0.25 ML), we find that hydrogen adsorbs in fourfold hollow sites on Rh(100), while at higher coverage the bridge site is preferred. Using Monte Carlo simulations, we unequivocally associate each surface component of the Rh $3d_{5/2}$ core level with a specific adsorption configuration. We obtain a value of 0.74 ± 0.08 for the hydrogen initial sticking coefficient, in very good agreement with previous reports.

DOI: 10.1103/PhysRevB.70.115404

PACS number(s): 68.43.Fg, 33.60.Fy

I. INTRODUCTION

The understanding of the hydrogen-metal interaction at a fundamental level is of primary relevance, since there is a great technological interest in the behavior of metal surfaces in the presence of hydrogen. As a clean energy vector, hydrogen is regarded as one of the most promising solutions to the environmental impact of the growing energy demand.^{1–3} Progress in the understanding of the interaction of hydrogen with metals is a fundamental step for the definition of the properties of materials needed for hydrogen production,⁴ storage,⁵ and final burning in fuel cells.³

The dissociative chemisorption of hydrogen on single crystal metal surfaces has been widely studied by means of both computational and experimental techniques.^{6–8} A considerable difficulty in the latter case is the limited sensitivity of conventional surface probes to the low scattering cross section of hydrogen atoms adsorbed on solid surfaces.^{7,9} Nevertheless, in specific cases, low energy electron diffraction (LEED), surface x-ray diffraction, He diffraction, ion scattering, and high resolution electron energy loss spectroscopy (HREELS) have been successfully applied for the determination of the hydrogen adsorption sites.⁷ Recently it has been also shown that scanning tunneling microscopy (STM) images can be misleading:¹⁰ the tip influences and actually drags the adsorbed hydrogen atoms into the bridge sites, showing an apparent coverage of 2 ML.

On Rh(100), dissociative hydrogen chemisorption has been extensively studied with conventional surface science probes.^{10–18} Desorption spectra after hydrogen saturation at 95 K show two peaks:¹¹ the most prominent at 330 K and an additional high coverage feature at 130 K. A desorption energy of 2.74 eV is found, which is almost constant up to about 0.8 ML, drastically decreasing for higher coverage. At saturation (0.9 ML), HREELS spectra¹¹ show a prominent feature at 82 meV which was attributed to the perpendicular

stretch mode for H adsorbed in the hollow site. A second feature, at 152 meV, was interpreted as the first overtone of the 82 meV vibration; a third, only partially resolved loss at 138 meV, was not clearly understood. At lower coverage (0.4 ML) only one feature at 70 meV is present. More recent higher resolution HREELS measurements¹² show that at intermediate coverage the spectra consist of a superposition of low-coverage losses and saturation (1.0 ML) losses. In particular, high-coverage features show up in the vibrational spectra already at 0.56 ML. Early density functional theory (DFT) calculations^{13,14} state that the adsorption energy difference between hollow and bridge sites for hydrogen on Rh(100) is 170 meV at 1 ML (neglecting zero point energies, which are of the order of 120 meV). More recent DFT results¹⁵ point out that the determination of the saturation coverage is nontrivial since the energy difference between possible adsorption sites is too small with respect to the calculation accuracy. It is found that repulsive lateral interactions between adsorbed atoms are reduced in islands of high coverage (up to 2 ML) bridge-bonded hydrogen. Most recent DFT calculations^{16,17} lead to the conclusion that, with the inclusion of the relativistic effects, the computed energy difference between the two competing adsorption sites is reduced to 40 meV, so that even zero point energies differences could become relevant in determining the preferred adsorption site. Experimentally, a quantitative LEED analysis¹⁰ reports a saturation coverage of 1.1 ± 0.6 ML at 120 K, with about 0.9 ML of hydrogen atoms in hollow sites and the remaining adsorbed in bridge positions, while accurate temperature desorption spectroscopy (TDS) yields a saturation coverage of 1.22 ML.^{10,18} In summary, divergences exist in the literature about the adsorption site and the saturation coverage of hydrogen on Rh(100), reflecting the experimental and theoretical difficulties described above.

In this paper we show that the analysis of the hydrogen-induced Rh $3d_{5/2}$ core level shifts provides a clear insight

into the coverage-dependence of the adsorption site for hydrogen on the Rh(100) surface. For the analysis, we successfully apply the adsorbate-induced surface core level shifts (SCLS) model recently proposed by our group.¹⁹ The results are complemented by Monte Carlo simulations based on the Unity Bond Index–Quadratic Exponent Potential (UBI-QEP) model developed by Shustorovich.^{20,21}

II. EXPERIMENTAL AND THEORETICAL BACKGROUND

A. Experimental setup

High resolution real-time fast x-ray photoelectron spectroscopy (XPS) experiments²² have been carried out at the SuperESCA beamline²³ of ELETTRA. The experimental chamber is equipped with a double pass 96-channel detector electron energy analyzer^{24,25} and a five-axis manipulator. Rh $3d_{5/2}$ core level spectra have been collected using photon energies from 393 up to 407 eV at an overall energy resolution of about 80 meV. The base pressure in the UHV experimental chamber was 1×10^{-10} mbar (residual gases consisting mainly of hydrogen and carbon monoxide). The sample was cooled by liquid nitrogen and heated by electron bombardment from a hot tungsten filament. It was cleaned following standard procedures by repeated Ar⁺ sputtering cycles, annealing to 1300 K, oxygen treatments and a final hydrogen reduction. Surface cleanliness was checked by measuring the C 1s and O 1s XPS signals, as well as by comparing the Rh $3d_{5/2}$ SCLS value for the clean surface with those reported in the literature.^{26–29} The hydrogen doses are expressed in Langmuir ($1 \text{ L} = 10^{-6} \text{ Torr s}$) and are corrected for the ion gauge sensitivity factor.

B. SCLS interpretation and data analysis

We attribute the different surface core level shifted components of the $3d_{5/2}$ experimental spectra to surface Rh atoms differently coordinated to hydrogen atoms, following a model recently proposed by our group.¹⁹ In this model a clear dependence of the shift of the surface component on the local adsorption structure is demonstrated on the basis of both experimental data analysis and DFT calculations. This behavior is determined by initial state effects related to the electronic environment of the system.³⁰ Final state contributions, which originate from the core hole screening, need to be considered for a precise and quantitative characterization of SCLS values.³¹ However, both experimental and DFT calculations have shown that for Rh(100) initial state effects dominate.^{19,29} In the present study we therefore use this assumption. Within the framework of this model, the energy shift $\Delta E_{i,j}$ (with respect to the position of the clean surface component) of the surface core level of a substrate atom bound to i atoms adsorbed in j -fold site symmetry, can be expressed as

$$\Delta E_{i,j} = i \times \Delta E_{1,j}. \quad (1)$$

This shows the additivity of the energy shift of a core level, which is caused by the single contributions of different “fractions” of adsorbate atoms. Similarly, a metal atom bound to

an adsorbate with coordination number j displays a shift given by

$$\Delta E_{1,j} = \frac{1}{j} \times \Delta E_{1,1}. \quad (2)$$

The Rh $3d_{5/2}$ core level spectra have been fitted, after linear background subtraction, with Doniach-Sunjić line shapes convoluted with a Gaussian function.³² The former is described by two parameters, the Anderson singularity index α , correlated to the final state screening, and the Lorentzian width Γ , which depends on the core hole lifetime.^{26,32} In the fitting procedure, the α and Γ parameters for the bulk, first and second layer peaks were initially fixed at the values previously found for the same surface.²⁶ The Gaussian contribution was allowed to vary in the least square fitting procedure, since its value depends on the energy resolution, surface temperature and surface inhomogeneity. In a second step, for each experimental condition (i.e., photon energy, energy-resolution, and photoelectron emission angles), all the fitting parameters were released for the clean surface spectra, yielding the “best fit” values, which were then used for deconvoluting the hydrogen uptake and desorption data.

C. UBI-QEP model

In order to describe the modifications of the surface layer during the hydrogen uptake and link them to the evolution of the observed core level components, we performed Monte Carlo simulations, in the framework of the UBI-QEP (Unity Bond Index–Quadratic Exponent Potential) model proposed by Shustorovich and Sellers.^{20,21} This model allows us to evaluate the adsorption energy of atoms adsorbed on single crystal metal surfaces as a function of coordination, taking into account their indirect, substrate-mediated lateral interactions. Briefly, it is based on the assumption that the single minimum pairwise interaction potential can be written as a polynomial function of a quantity which is called the bond index x_j . In an n -fold coordinated adsorption site, the n two-body bond indexes are defined as

$$x_j(r_j) = \sum_i c_i e^{(r_j - r_0)/b_i}, \quad j = 1, \dots, n, \quad \sum_i c_i = 1, \quad (3)$$

where $r_{0,j}$ is the equilibrium distance for the j th bond; b_i and c_i are parameters defining the shape of the potential. The multibody potential energy can be written as the sum of the nearest neighbor pairwise interactions, imposing the unity conservation of the total bond index,²¹

$$X = \sum_j x_j(r_j) = 1. \quad (4)$$

Using these assumptions, it is found that the binding energy of an adsorbate A in an n -fold adsorption site is given by

$$Q_{nA} = Q_{0A} \left(2 - \frac{1}{n} \right), \quad (5)$$

where Q_{0A} is the heat of adsorption in the on-top site. The local atomic heat of adsorption as a function of the coverage can also be obtained by applying the conservation of the

bond index. For an adsorbate atom A in an n -fold site one obtains

$$Q_{nA}(\theta) = Q_{nA} \frac{1}{n} \sum_i \frac{k_i}{m_i} \left(2 - \frac{1}{m_i} \right), \quad (6)$$

where k_i is the number of surface metal atoms of type i bound to m_i adsorbates.

The only input of our simulations is the adsorption energy of hydrogen on Rh(100) calculated by DFT in the zero coverage limit.^{10,16,17} Monte Carlo simulations have been performed on a (15×15) unit cell with periodic boundary conditions. The dimension of the unit cell was selected in order to minimize border effects and to allow reasonable computation times: even simulations performed on (10×10) and (12×12) cells did not show substantial differences. For each selected surface coverage θ_n , the hydrogen uptake was performed randomly with no discrimination between the four-fold and bridge adsorption sites. Equilibration of the system was always reached within 5000 MCS (Monte Carlo Steps); in each of the MCS, $\theta_n \times 15 \times 15$ hydrogen atoms were randomly chosen, the hopping direction was randomly selected and finally the hopping probability was calculated for each of the selected adsorbate atoms. The site occupancy probability was calculated using the Boltzmann distribution, the adsorption energies for each local configuration were calculated using the UBI-QEP model and the hopping process was controlled by the Metropolis algorithm. Simulations have been carried out at final temperatures ranging from 60 to 200 K, using simulated annealing equilibration. No differences have been observed between single- or multiple-hopping kinetics, nor between independent or sequential uptakes (i.e., starting for each increasing coverage from the clean surface or adding extra hydrogen to the previous equilibrated configuration). The reliability of our code was checked by reproducing the results obtained by Hansen and co-workers³³ for oxygen adsorption on the Rh(100) surface up to 0.5 ML. Our simulations for hydrogen were performed only up to a surface coverage of 0.6 ML, as the UBI-QEP model is known to fail at high concentrations, due to overestimation of the adsorption and interaction energies.²¹

III. RESULTS

A. Experiment

High resolution time-resolved XPS spectra of the Rh $3d_{5/2}$ core level were collected during hydrogen uptake at several temperatures between 70 and 140 K: no differences were detected within this range. For the clean surface (see Fig. 1) three contributions have been identified and assigned to bulk, first-, and second-layer atoms, respectively. The clean surface first-layer peak (R_s) is positioned at -626 ± 5 meV from the bulk peak (R_b). A second-layer contribution, revealed also on Rh(111),³⁴ is centered at $+75 \pm 10$ meV, in agreement with previous findings.³⁵ The “best fit” parameter values are $\Gamma_b = 0.23$ eV and $\alpha_b = 0.27$, $\Gamma_s = 0.28$ eV and $\alpha_s = 0.20$, $\Gamma_{2nd \text{ layer}} = 0.19$ eV and $\alpha_{2nd \text{ layer}}$

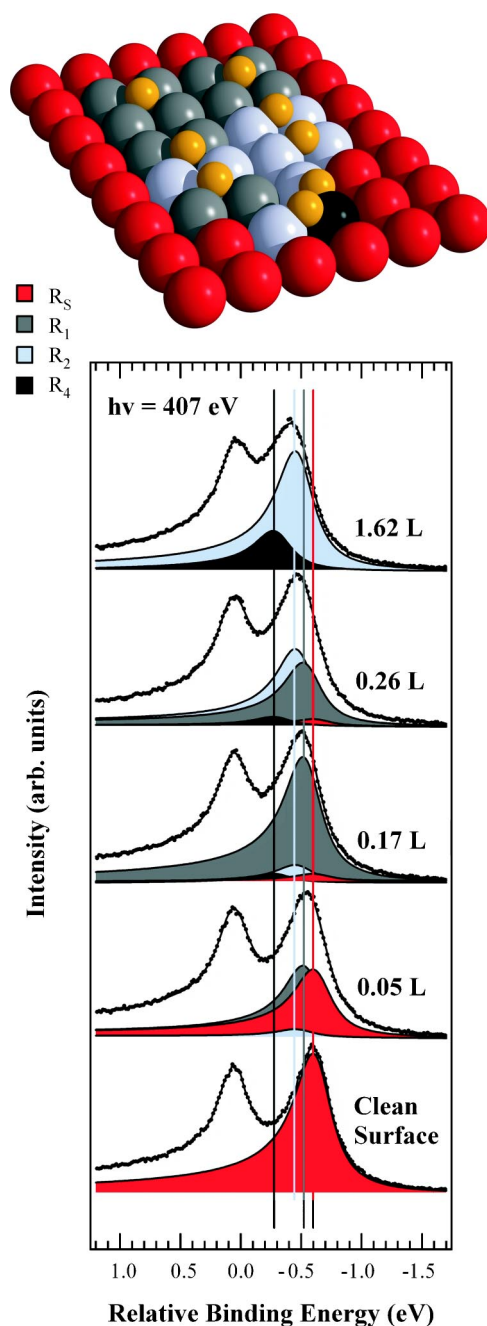


FIG. 1. (Color online) Selected Rh $3d_{5/2}$ spectra collected during the hydrogen uptake at 150 K ($h\nu=407$ eV). The several contributions to the surface peak shape are shown. The binding energy scale is referred to the bulk component position. Bulk and second-layer components are not shown.

$= 0.10$, for the bulk, first and second layer, respectively. Again these values are in good agreement with those previously reported.²⁶

During the hydrogen uptake, the clean surface Rh $3d_{5/2}$ component progressively vanishes, while new components grow at higher binding energies, closer to the bulk peak (see Fig. 1). By least square fitting we find three other surface related peaks, positioned at -547 ± 5 meV (R_1), -481 ± 5 meV (R_2), and -308 ± 5 meV (R_4) from the bulk peak, respectively. Alternatively, if we measure their position

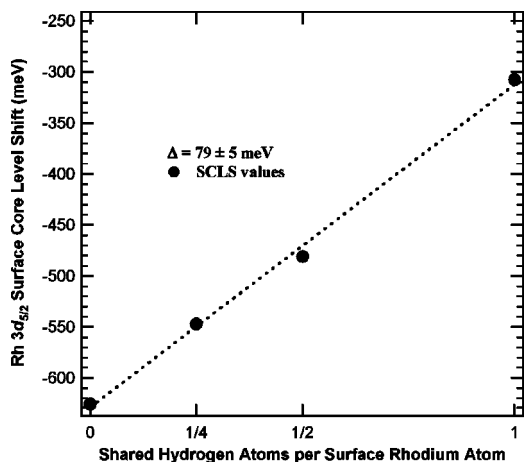


FIG. 2. Rh $3d_{5/2}$ peak positions with respect to the bulk component, associated to the nonequivalent surface rhodium species. The linear fit to obtain the value for the quantization of the SCLS displacement (Δ) is shown.

with reference to the clean surface peak, the new features are centered at Δ , 2Δ , and 4Δ respectively, assuming for Δ a value of 79 ± 5 meV (see Fig. 2). Interestingly, the “ 3Δ ” SCLS component is absent from the spectra; even forcing a peak at this position, its intensity goes to zero during the fitting procedure.

Using our SCLS model,¹⁹ we can attribute the different surface components to specific bonding geometries: in particular, the peak R_1 centered at $\Delta = \Delta E_{1,4}$ can be associated with surface rhodium atoms bound to a single hydrogen atom adsorbed in a fourfold site. Analogously, the peak R_2 at $2\Delta = \Delta E_{2,4} = \Delta E_{1,2}$ can be attributed to rhodium atoms bound to two hydrogen atoms in fourfold sites or, equivalently, to rhodium atoms bonded to single hydrogen atoms in bridge sites. Finally, the feature R_4 at $4\Delta = \Delta E_{4,4} = \Delta E_{2,2}$ corresponds to surface atoms bound to four hydrogen atoms in hollow sites or to rhodium atoms bound to two hydrogen atoms in bridge positions (see Fig. 3).

Analyzing the behavior of the peak intensities as a function of the hydrogen exposure (see Fig. 4), it can be observed

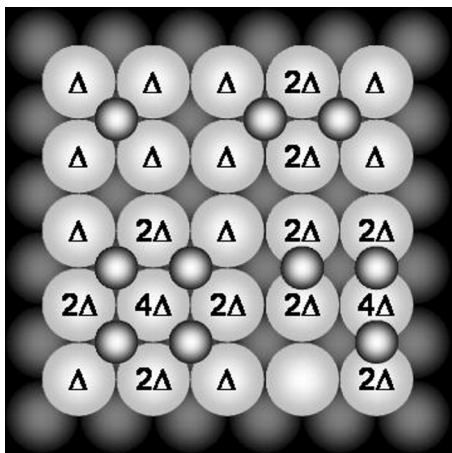


FIG. 3. Surface model showing the classification of the nonequivalent first-layer rhodium atom species: $\Delta = \Delta E_{1,4}$, $2\Delta = \Delta E_{2,4} = \Delta E_{1,2}$, $4\Delta = \Delta E_{4,4} = \Delta E_{2,2}$.

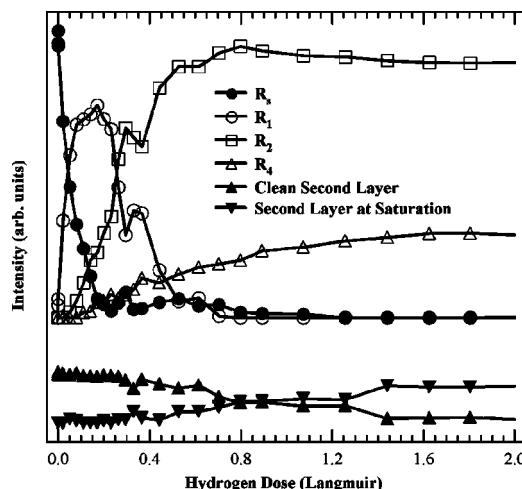


FIG. 4. Intensities of the Rh $3d_{5/2}$ surface and second-layer core level components as a function of hydrogen exposure at 120 K ($h\nu = 407$ eV). The first-layer features are associated to the nonequivalent surface rhodium species (Ref. 19); R_5 —clean surface; R_1 — Δ ; R_2 — 2Δ ; R_4 — 4Δ .

that the contribution of R_s vanishes at about 0.2 L, but grows back again around 0.5 L. As previously reported,¹² hydrogen saturation is reached at about 2 L; at this coverage only two surface first-layer components (R_2 and R_4) are present. During the whole uptake experiment the intensity of the R_b component remains almost constant. Besides the hydrogen related components, a new second-layer core level shifted component appears at $+48 \pm 10$ meV with respect to the bulk feature in the XPS spectra (see Fig. 4). This component sets in above 0.1 L and grows up to saturation at the expenses of the clean surface second layer contribution centered at $+75 \pm 10$ meV, which vanishes at saturation. A similar behavior for the second-layer component has already been reported for hydrogen adsorption on W(100),³⁶ where a hydrogen-induced restructuring was involved.

At the end of each hydrogen uptake experiment, we performed a desorption experiment by annealing the sample to a specific temperature with a rate of 5 K/s, following immediate cooling to 150 K and collecting the XPS spectra.

In Fig. 5 the behavior of the multiple core level shift components of the Rh $3d_{5/2}$ peak are reported as a function of the annealing temperature. The relative intensities of the surface components during desorption show the reversed behavior with respect to the uptake.

B. Monte Carlo simulations

We performed Monte Carlo simulations for increasing hydrogen coverage (in the 0.0–0.6 ML range with 0.025 ML steps) at 120 K. An adsorption energy difference between hollow and bridge sites of 40 meV and an adsorption energy of 2850 meV (Q_{4A}) (Ref. 37) for the zero-coverage limit in the fourfold site were assumed.^{10,16,17} In Fig. 6 the instantaneous configurations obtained after equilibration for selected adsorbate coverages are reported. At 0.25 ML almost all adsorbed atoms are in fourfold hollow sites. The small difference in the heat of adsorption between bridge and hollow

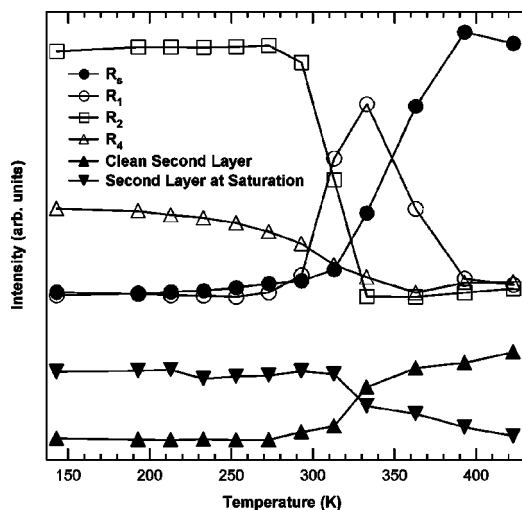


FIG. 5. Intensities of the Rh $3d_{5/2}$ surface and second-layer core level components as a function of the annealing temperature. All spectra were collected at a temperature of 120 K ($h\nu=407$ eV). The first-layer features are associated to the nonequivalent surface rhodium species (Ref. 19); R_5 —clean surface; R_1 — Δ ; R_2 — 2Δ ; R_4 — 4Δ .

sites allows occasional occupation of the bridge sites, which decreases when the surface temperature in the simulations is lowered. Accordingly, the surface rhodium atoms are mainly of “ Δ ” type (see Fig. 3). As the hydrogen coverage increases, the lateral interactions progressively make it more energetically convenient to populate bridge sites. During this process, “ 2Δ ” rhodium atoms become predominant (as can be seen in Fig. 6 for the 0.35 ML surface), while some surface atoms remain free from adsorbed hydrogen atoms. This effect accounts remarkably well for the growth of the R_s peak at 0.5 L during the uptake (see Fig. 4). At coverages higher than 0.5 ML (see Fig. 6), all hydrogen atoms are in bridge sites, which gives rise to “ 2Δ ” Rh atoms and, at the highest

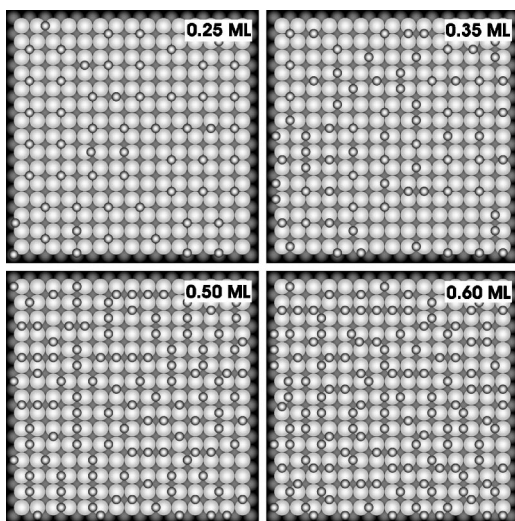


FIG. 6. Selected structural models of the equilibrium configurations obtained by Monte Carlo simulations during hydrogen uptake. Unit cell dimensions: 15×15 ; final simulation temperature: 120 K; nMCS: 5000.

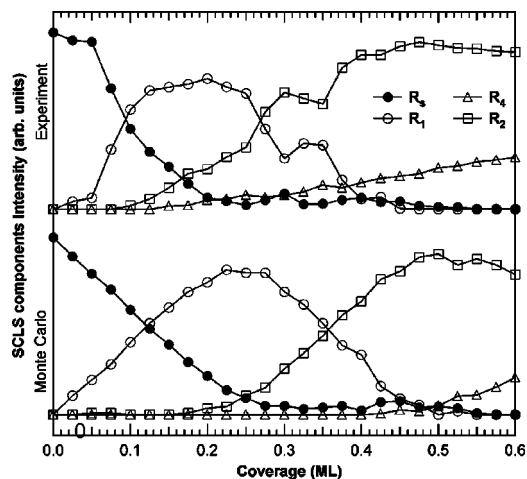


FIG. 7. Comparison between experimental and simulation curves for the SCLS components as a function of surface coverage; R_5 —clean surface; R_1 — Δ ; R_2 — 2Δ ; R_4 — 4Δ .

examined coverage (0.6 ML), also to “ 4Δ ” surface atoms (i.e., atoms which are bonded to two adsorbate atoms in bridge sites). In agreement with the experiments, none of the simulations show the presence of “ 3Δ ” atoms, which require higher values of the adsorption energy difference between the bridge and hollow sites (>80 meV).

The relative SCLS intensity for each surface configuration is simply assumed to be proportional to the population of each Rh surface species; the final values for each equilibrated system, obtained upon averaging over the last 500 MCS of each simulation, are reported in Fig. 7, bottom panel.

IV. DISCUSSION

From data analysis we understand that no “ 3Δ ” Rh atoms are ever generated during the uptake and that two inequivalent Rh surface atoms are present at saturation: at coverages lower than 0.25 ML only fourfold hollow sites are occupied, while for higher coverages hydrogen preferentially adsorbs in bridge sites. It is remarkable to compare the results of the SCLS analysis with the output of the Monte Carlo simulations. They both yield the hydrogen adsorption site population, but the former as a function of the hydrogen exposure, while the latter related to the surface coverage.

Assuming a second order process, we express the adsorption rate as

$$r = \frac{d\theta_H}{dt} = 2 \frac{d\theta_{H_2}}{dt} = \frac{2p_{H_2}s_0 \left(1 - \frac{\theta_H}{\theta_s}\right)^2}{\sqrt{2\pi m_{H_2} k_B T}}, \quad (7)$$

where p_{H_2} is the molecular hydrogen gas pressure, s_0 the initial sticking coefficient, θ_s the surface saturation coverage, k_B the Boltzmann constant, and T the gas temperature. By integrating Eq. (7) we obtain a direct relationship between surface coverage and exposure as a function of two unknown parameters only: s_0 and θ_s . We performed a fitting procedure,

obtaining the values of s_0 and θ_s which produce the best agreement between experiment and simulations. Figure 7 (top) shows the experimental data plotted vs coverage, which now can be directly compared with the results reported in Fig. 7 (bottom), evidencing a remarkable agreement. All the features of the simulations are present in the experimental data, even the persisting intensity of the clean surface component above 0.3 ML, linked to the change in the adsorption site (from hollow to bridge).

From the fit, we obtain for s_0 a value of 0.74 ± 0.08 , in good agreement with the theoretical value of 0.8 (Ref. 38) and the recent experimental value of 0.85 ± 0.15 .¹⁸ Moreover, we find a saturation coverage limit of 0.80 ± 0.07 ML: this is compatible with the value of 1.1 ± 0.6 ML (Ref. 10) and very close to the value of 0.9 ML reported in Ref. 11, while it is in contrast with the value of 1.22 ML determined by TPD calibration.^{10,18}

V. CONCLUSIONS

By comparing the results of SCLS analysis of the Rh $3d_{5/2}$ core level with UBI-QEP Monte Carlo simulations, the adsorption sites of hydrogen on Rh(100) at low temperature have been determined as a function of surface coverage. We have shown that at low coverage hydrogen prefers the most coordinated hollow site, whereas at increasing densities, the bridge site becomes energetically preferred due to substrate mediated lateral interactions.

ACKNOWLEDGMENTS

We thank A. Eichler, A. Winkler, and D. Menzel for helpful discussions. Financial support has been provided by MIUR, under the program "PRIN2001," Contract No. 2001023192.

-
- ¹J. M. Ogden, *Phys. Today* **55**, 69 (2002).
²M. Schrope, *Nature (London)* **414**, 682 (2001).
³P. Hoffmann, *Tomorrow's Energy* (MIT Press, Cambridge, 2001).
⁴J. H. Larsen and I. Chorkendorff, *Surf. Sci. Rep.* **35**, 163 (1999).
⁵M. D. Ward, *Science* **300**, 1104 (2003).
⁶K. Christmann, *Surf. Sci. Rep.* **9**, 1 (1999).
⁷H. Over, *Prog. Surf. Sci.* **58**, 249 (1998).
⁸J. W. Davenport and P. J. Estrup, *The Chemical Physics of Solid Surfaces and Heterogenous Catalysis* (Elsevier, New York, 1990), Vol. 3, p. 33.
⁹J. V. Barth, *Surf. Sci. Rep.* **40**, 75 (2000).
¹⁰C. Klein, A. Eichler, E. L. D. Hebenstreit, G. Pauer, R. Koller, A. Winkler, M. Schmidt, and P. Varga, *Phys. Rev. Lett.* **90**, 176101 (2003).
¹¹L. J. Richter and W. Ho, *J. Vac. Sci. Technol. A* **5**, 453 (1987).
¹²L. J. Richer, T. A. Germer, J. P. Sethna, and W. Ho, *Phys. Rev. B* **38**, 10 403 (1988).
¹³D. R. Hamann and P. J. Feibelman, *Phys. Rev. B* **37**, 3847 (1988).
¹⁴P. J. Feibelman, *Phys. Rev. B* **43**, 9452 (1991).
¹⁵S. Wilke, D. Hennig, and R. Löber, *Phys. Rev. B* **50**, 2548 (1994).
¹⁶A. Eichler, J. Hafner, and G. Kresse, *J. Phys.: Condens. Matter* **8**, 7659 (1996).
¹⁷A. Eichler, J. Hafner, and G. Kresse, *Surf. Rev. Lett.* **4**, 1297 (1997).
¹⁸G. Pauer, A. Eichler, M. Sock, M. G. Ramsey, F. Netzer, and A. Winkler, *J. Chem. Phys.* **119**, 5253 (2003).
¹⁹A. Baraldi, S. Lizzit, G. Comelli, M. Kiskinova, R. Rosei, K. Honkala, and J. K. Nørskov, *Phys. Rev. Lett.* **93**, 046101 (2004).
²⁰E. Shustorovich, *Surf. Sci. Rep.* **6**, 1 (1986).
²¹E. Shustorovich and H. Sellers, *Surf. Sci. Rep.* **31**, 1 (1998).
²²A. Baraldi, G. Comelli, S. Lizzit, M. Kiskinova, and G. Paolucci, *Surf. Sci. Rep.* **49**, 169 (2003).
²³A. Baraldi, M. Barnaba, B. Brena, D. Cocco, G. Comelli, S. Lizzit, G. Paolucci, and R. Rosei, *J. Electron Spectrosc. Relat. Phenom.* **76**, 145 (1995).
²⁴A. Baraldi and V. R. Dhanak, *J. Electron Spectrosc. Relat. Phenom.* **67**, 211 (1994).
²⁵L. Gori, R. Tommasini, G. Cautero, D. Giuressi, M. Barnaba, A. Accardo, S. Carrato, and G. Paolucci, *Nucl. Instrum. Methods Phys. Res. A* **431**, 338 (1999).
²⁶A. Baraldi, G. Comelli, S. Lizzit, R. Rosei, and G. Paolucci, *Phys. Rev. B* **61**, 12 713 (2000).
²⁷K. C. Prince, B. Ressel, C. Astaldi, M. Peloi, R. Rosei, M. Polcik, C. Crotti, M. Zacchigna, C. Comicioli, C. Ottavini, C. Quaresima, and P. Perfetti, *Surf. Sci.* **377**, 117 (1997).
²⁸A. Borg, C. Berg, S. Raaen, and H. J. Venvik, *J. Phys.: Condens. Matter* **6**, L7 (1994).
²⁹J. N. Andersen, D. Hennig, E. Lundgren, M. Methfessel, R. Nyholm, and M. Scheffler, *Phys. Rev. B* **50**, 17 525 (1994).
³⁰N. Mårtensson and A. Nilsson, *Applications of Synchrotron Radiation*, Springer Series in Surface Sciences, edited by W. Eberhardt (Springer, Berlin, 1995), Vol. 35, p. 65.
³¹M. V. Ganduglia-Pirovano, M. Scheffler, A. Baraldi, S. Lizzit, G. Comelli, G. Paolucci, and R. Rosei, *Phys. Rev. B* **63**, 205415 (2001).
³²S. Doniach and M. Sunjic, *J. Phys. C* **3**, 185 (1970).
³³E. W. Hansen and M. Neurock, *Surf. Sci.* **464**, 91 (2000).
³⁴A. Baraldi, S. Lizzit, A. Novello, G. Comelli, and R. Rosei, *Phys. Rev. B* **67**, 205404 (2003).
³⁵A. Baraldi, S. Lizzit, A. Novello, G. Comelli, and R. Rosei (unpublished).
³⁶J. Puppelle, K. G. Purcell, and D. A. King, *Surf. Sci.* **367**, 149 (1996).
³⁷A. Eichler (private communication).
³⁸A. Eichler, J. Hafner, A. Groß, and M. Scheffler, *Phys. Rev. B* **59**, 13 297 (1999).